Specific Drug Delivery to Cancer Cells with Double-Imprinted Nanoparticles against Epidermal Growth Factor Receptor

Francesco Canfarotta,[▽,†] Larissa Lezina,[▽,‡,∥] Antonio Guerreiro,[†] Joanna Czulak,[†] Alexey Petukhov,[∥,⊥] Alexandra Daks,[∥] Katarzyna Smolinska-Kempisty,[§] Alessandro Poma,[#] Sergey Piletsky,[*] and Nickolai A. Barlev[,∥,○]*

[†] MIP Diagnostics Ltd., Fielding Johnson Building, Leicester, LE1 7RH United Kingdom

[‡] Department of Cancer Studies and § Department of Chemistry, University of Leicester, Leicester, LE1 7RH United Kingdom

[∥] Laboratory of Gene Expression and Regulation, Institute of Cytology, 194064 Saint Petersburg, Russia

[⊥] Institute of Hematology, Almazov National Medical Research Centre, 197341 Saint Petersburg, Russia

[#] Chemistry Department, University College London, London, WC1H 0AJ United Kingdom

[○] Moscow Institute of Physics and Technology, Dolgoprudny, Moscow Oblast, 141700 Russia

Molecular imprinting, nanoparticles, molecular recognition, membrane receptors, cancer, drug delivery

ABSTRACT. Epidermal growth factor receptor (EGFR), a tyrosine kinase receptor, is over-expressed in many tumors, including almost half of triple-negative breast cancers. The latter belong to a very-aggressive and drug-resistant form of malignancy. Although humanized anti-EGFR antibodies can work efficiently against these cancers both as monotherapy and in combination with genotoxic drugs, instability and high production costs are some of their known drawbacks in clinical use. In addition, the development of antibodies to target membrane proteins is a very challenging task. Accordingly, the main focus of the present work is the design of supramolecular agents for the targeting of membrane proteins in cancer cells and, hence, more-specific drug delivery. These were produced using a novel double-imprinting approach based on the solid-phase method for preparation of molecularly imprinted polymer nanoparticles (nanoMIPs), which were loaded with doxorubicin and targeted toward a linear epitope of EGFR. Additionally, upon binding, doxorubicin-loaded anti-EGFR nanoMIPs elicited cytotoxicity and apoptosis only in those cells that over-expressed EGFR. Thus, this approach can provide a plausible alternative to conventional antibodies and sets up a new paradigm for the therapeutic application of this class of materials against clinically relevant targets. Furthermore, nanoMIPs can promote the development of cell imaging tools against difficult targets such as membrane proteins

Protein−protein interactions are central to most biological processes from intercellular communication to programmed cell death and represent a large and important class of targets for human therapeutics. The current excitement around therapeutic antibodies vividly illustrates the value of such targets, with a market value predicted to reach $125 billion USD by 2020.[1] As a compound class, antibodies are highly specific for their molecular antigen and are usually stable in human serum. However, antibodies suffer from complex manufacturing procedures, high production costs, lack of oral bioavailability, poor cell membrane permeability, and increased patient morbidity, and even humanized types can elicit immunogenic reactions.[1−5] Also, while cell surface receptors are obvious antigens when attempting to target specific cell populations, in practice, obtaining antibodies against such receptors is a very challenging task.[6,7] In this article, we assess the potential of molecularly imprinted polymer nanoparticles (nanoMIPs) as an alternative to antibodies against cell membrane receptors and their potential in cell imaging and targeted drug delivery.

When produced in nanoparticle format,[8] MIPs exhibit a size compatible with biological applications and, therefore, can be used for labeling and targeting specific cell structures. Also, these nanoparticles can plausibly become a new class of therapeutic agent, which can address both extracellular protein targets as well as intracellular proteins[9] (currently inaccessible to antibodies). The nanoMIPs were produced using a solid-phase double-imprinting approach against two targets, a linear epitope of the extracellular domain of the epidermal growth factor receptor (EGFR) and against the cytotoxic agent doxorubicin. Consequently, nanoMIPs are capable of selectively recognizing EGFR-over-expressing cells while possessing, at the same time, binding sites for loading the cytotoxic agent doxorubicin. EGFR was selected as target

protein because it is over-expressed in several malignancies, including breast, colorectal, and lung cancers, and is one of the critical regulators of cell proliferation and invasiveness.[10–13]

The solid-phase method employed for the MIP preparation (**Figure 1a**) relies on the covalent immobilization of the primary template (a synthetic short EGFR peptide) on a solid support (e.g., glass beads).

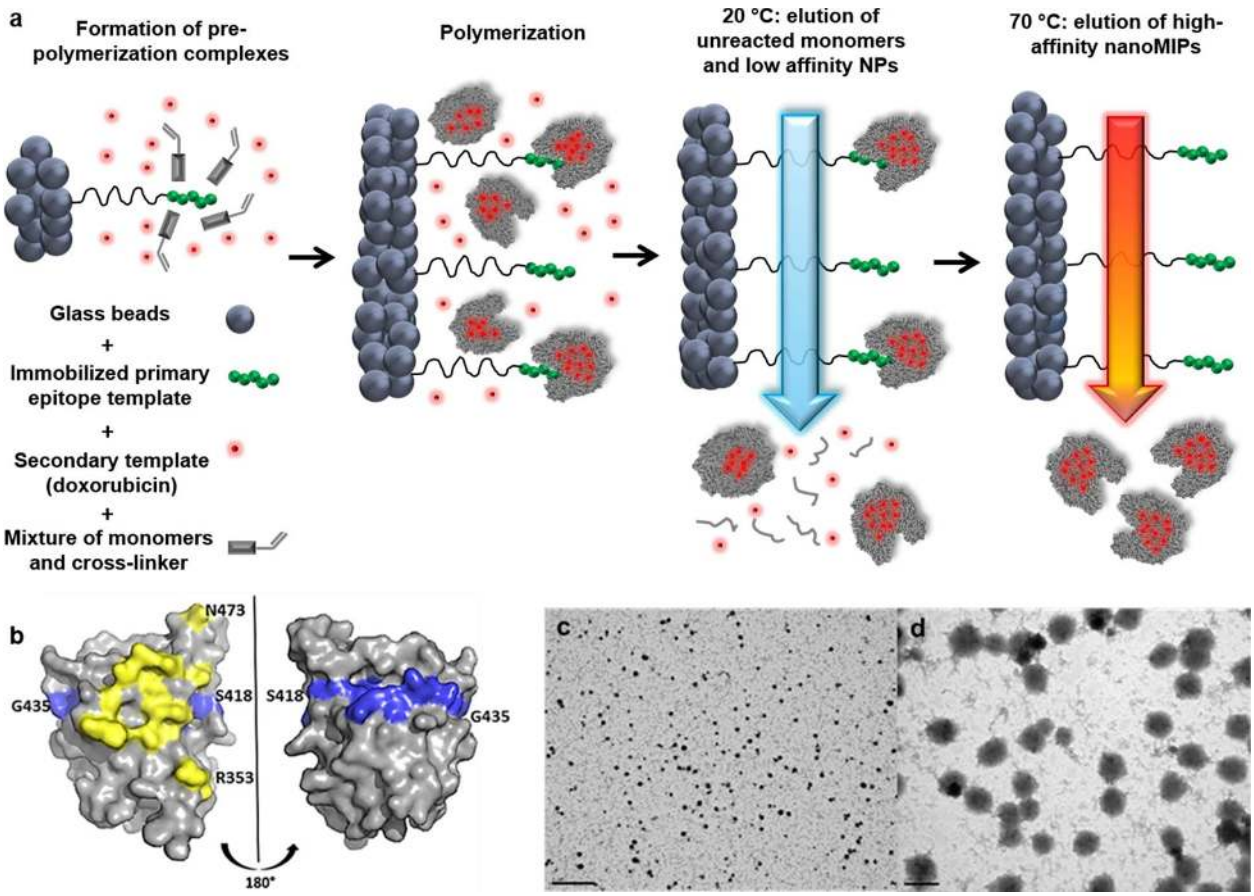

Figure 1. (a) Scheme of the solid-phase synthesis process for double-imprinted nanoMIPs using a peptide epitope of EGFR as primary template attached to the solid phase and doxorubicin as secondary template in solution. (b) The 3D structure of EGFR shown in blue is the sequence of the peptide template used for nanoMIPs fabrication, and the antigenic region for the therapeutic antibody cetuximab, which targets the same receptor, is shown in yellow. (c, d) TEM images of

EGFR nanoMIPs at (c) 20 000× magnification and (d) 80 000× magnification. Scale bars are, respectively, 1 μm and 200 nm.

This support bearing the immobilized template is placed in contact with the monomer mixture, which also contains the drug to be incorporated (doxorubicin) as a secondary template in solution, then polymerization is initiated under conditions that promote the formation of polymer nanoparticles (**Figure 1c,d**). NanoMIPs obtained in this way are surface-imprinted against the primary template for accurate cell targeting while possessing binding sites within their bulk for drug delivery (**Figure 1a**). The products obtained using this method are virtually free from the primary template (as it is immobilized),[8,14,15] whereas other traditional production approaches require lengthy dialysis of the nanoMIPs to remove it.[16,17] NanoMIPs with homogeneous binding affinities, nanomolar dissociation constants, and good specificity for all major target classes (from small molecules to peptides and proteins) have been produced by solid-phase imprinting[16,18,19] and used in the development of sensors and assays.[20–24]

Whereas the common approach to specifically target cancer cells is exerted via antibodies,[25] very recently, other research groups employed nanoMIPs to target over-expressed moieties exposed on the surface of cells. However, only saccharides (sialic and glucuronic acid) have been used as templates for the successful generation of MIPs.[26–28] Here, anti-EGFR nanoMIPs (EGFR-MIPs) were produced against a synthetic C-terminal linear peptide sequence (amino acids 418−435: SLNITSLGLRSLKEISDG) of the extracellular portion of the EGFR receptor (PDB ID: 1NQL), which is exposed at the protein surface (**Figure 1b**). A cysteine residue was added on the N-terminus of the epitope to allow its oriented immobilization on the solid-phase through a thiol-reactive linker prior to nanoMIPs synthesis (see the Experimental section of the Supporting Information for full details). The use of synthetic peptide epitopes as templates to

produce imprinted polymers against proteins with a known sequence is potentially a novel and generic method that features significant advantages because it does not require the preparation and purification of the full-length proteins, which are often difficult to produce in sufficient quantities, are unstable, or both.

To produce nanoMIPs, a mixture of monomers previously optimized specifically to imprint peptides and proteins in a mild aqueous conditions was employed.[15,17,29] The solid phase bearing the immobilized primary template was placed in contact with the monomer mixture (which contained the secondary template) and free-radical precipitation polymerization was initiated. Various monomers capable of establishing different molecular interactions with the epitope template were selected; these included: *N*-isopropylacrylamide (hydrogen bonding), *N*-*tert*-butylacrylamide (hydrophobic interactions), acrylic acid, and *N*-(3-aminopropyl)methacrylamide (ionic interactions), while *N,N′*-methylenebis(acrylamide) was used as a cross-linker. Due to the range of monomers used, this composition is also appropriate to imprint smaller molecules;[18] therefore, the secondary template (doxorubicin) was simply added to the polymerization mixture. To visualize the nanoMIP interaction with the cancer cells, a fluorescent monomer, *N*-fluoresceinylacrylamide (*N*-fluo), was added to the monomer solution (see **Figure S1** for the fluorescence spectra).

After polymerization, EGFR-nanoMIPs were obtained with an average hydrodynamic diameter in deionized water of 242 ± 13 nm, as measured by dynamic light scattering (DLS) and with approximately 150−200 nm when measured in the dry state by TEM (see **Figures S1, S2,** and **1c,d**). NanoMIPs were tested by surface plasmon resonance (SPR) to determine their affinity toward the primary template (the EGFR peptide epitope) as well as for the extracellular part oft he EGFR protein (aa 1−641). For control experiments, biotin-imprinted nanoparticles were

prepared with the same monomer composition. Biotin was used as the template because non-imprinted materials cannot be produced using the solid-phase approach (the affinity separation step cannot be performed in the absence of an immobilized template). Biotin is sufficiently different from the EGFR epitope and is not naturally exposed on the cell surface, so these nano-MIPs can be considered for practical purposes as non-EGFR-imprinted materials. An equilibrium dissociation constant (K_D) of 7.7 nM was obtained for the EGFR-nanoMIPs binding to the peptide, while a K_D of 3.6 nM was obtained for the binding to the extracellular domain of the EGFR protein. Practically no binding of the EGFR peptide could be observed on the control nanoparticles (see **Figure S3** for the sensorgrams).

To assess the efficacy of EGFR-nanoMIPs binding to their target region of EGFR in live cells, three breast cancer cell lines expressing different levels of EGFR (assessed by Western blot; **Figure 2a**) were incubated with *N*-fluo-labeled nanoMIPs, followed by flow cytometry (FACS) analysis (**Figure 2b,c**). From the results shown in Figure 2 the breast cancer MDAMB-468 cells, which expressed the highest amount of EGFR, also exhibited the highest binding of EGFR-nanoMIPs (**Figure 2c**). Conversely, SKBR3 cells (that expressed virtually no EGFR) did not show any appreciable binding by the EGFR-nanoMIPs. To further assess the binding of fluorescent EGFR-nanoMIP, automated confocal microscopy was performed on MDA-MB-468 and SKBR-3 cells, respectively, expressing high and low levels of EGFR (**Figure 2d,e**). The nucleus was stained with DAPI (blue), and γ-tubulin (red) was employed to stain cell membrane. *N*-fluo-EGFR-nanoMIPs show green emission around 510 nm (**Figure S4**). In agreement with the results obtained by FACS, we detected a strong fluorescent signal from the MIPs in MDA-MB-468 cells over-expressing EGFR (**Figure 2e**), whereas almost no signal was observed in MDA231 or SKBR3 cells (**Figures 2d** and **S5**).

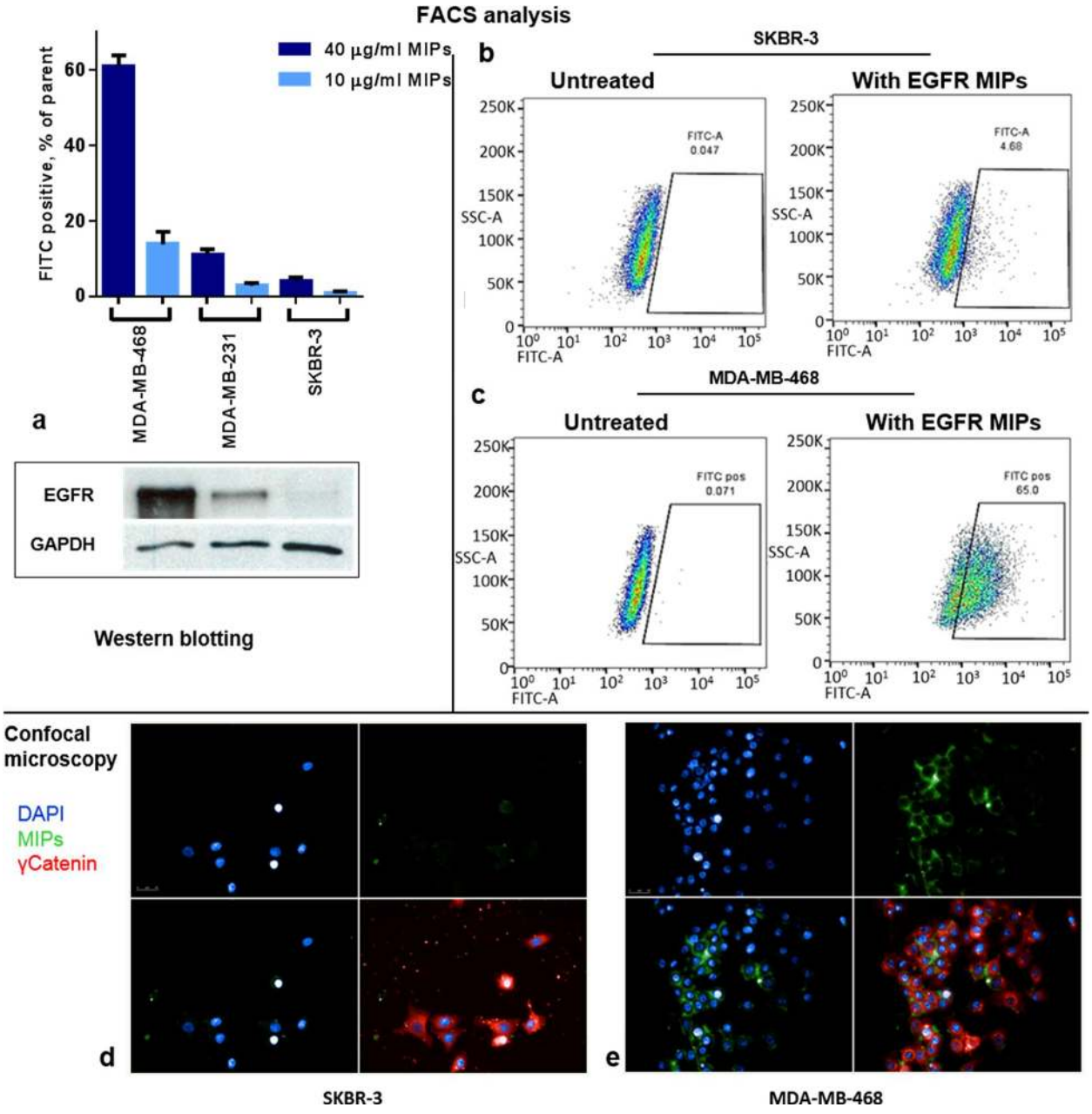

Figure 2. Analysis of binding specificity for fluorescent *N*-fluo-EGFR-nanoMIPs in breast cancer cells. (a) FACS analysis of binding of EGFR-nanoMIPs to three cell lines expressing different levels of EGFR. Bars represent standard deviation for three replicates. FACS analysis on (b) SKBR-3 (expressing low amounts of EGFR) and (c) MDA-MB-468 cells (expressing high amounts of EGFR), demonstrating binding of EGFRnanoMIPs to be proportional to amount of

EGFR. Confocal microscopy on (d) SKBR-3 and (e) MDA-MB-468 cells, confirming the specific binding of EGFR-nanoMIPs (green) to the target protein.

To further demonstrate that EGFR-nanoMIPs bind specifically to the protein epitope in live cells, a competition assay with free peptide epitope in solution (tested at 10-fold range of concentrations: 0.1 and 1 μM) was performed using MDAMB-468 cells (**Figure S6**). The results showed a significant reduction of the amount of cell-bound EGFR-nanoMIPs detected by flow cytometry.

However, the free peptide could not completely abolish the nanoMIP binding to the cells, arguing that some of the MIPs bind their target irreversibly. This is also suggested by the slow K_{OFF} of the nanoMIPs bound to the EGFR protein, as detected by SPR (**Figure S3**). Importantly, the presence of the same peptide in the binding assay performed with SKBR-3 cells expressing low amount of EGFR had no obvious effect on already minuscule binding of EGFR-MIPs (compare the right panel of Figure S6). Taken together, this indicates that EGFR-MIPs bind the EGFR epitope in a selective and competitive fashion. Collectively, these results demonstrate that the synthesized EGFR-nanoMIPs are specific for EGFR under physiological conditions, highlighting the potential use of nanoMIPs as convenient imaging tools to target specific membrane proteins in specific cell populations.

Next, by employing EGFR-nanoMIPs, we explored the possibility of delivering a cytotoxic drug (doxorubicin) specifically to MDA-MB-468 cells enriched in EGFR. To this end, the drug was loaded into the double-imprinted EGFRnanoMIPs ("doxo-EGFR-nanoMIPs"). Because doxorubicin is a potent genotoxic drug, we expected that EGFR-expressing cells should preferentially be killed in comparison to cells treated with doxo-biotin-nanoMIPs, which cannot

deliver the drug specifically to the cancer cells. The level of cell death was monitored by MTS and FACS analyses. In these experiments, "unloaded" EGFR-nanoMIPs showed no cytotoxic effects, while doxo-loaded EGFR-nanoMIPs elicited an evident reduction in cell viability (**Figure 3a**). This effect was specific because SKBR-3 cells, which express low levels of EGFR, were insensitive to the treatment with doxo-loaded EGFR-nanoMIPs.

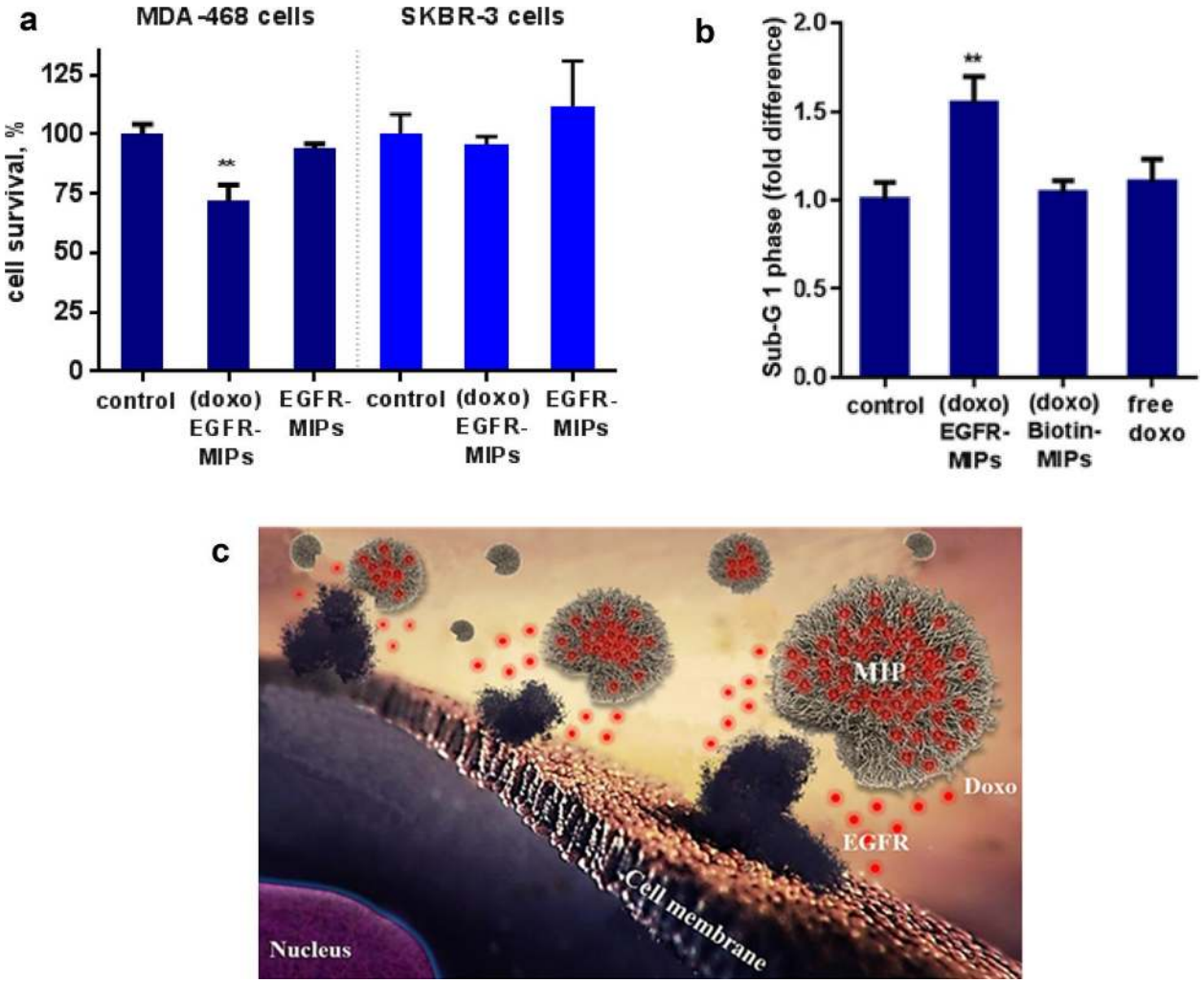

Figure 3. Toxicity assays. (a) MTS test performed on MDA-MB-468 and SKBR-3 cells treated with EGFR-nanoMIPs either loaded with doxorubicin (doxo-EGFR-MIPs) or unloaded (EGFR-MIPs). The control represents cells incubated in the absence of nanoMIPs. (b) Increase of the

level of MDA-MB-468 cells in the sub-G1 phase due to the binding of doxo-EGFR-nanoMIP and doxo-biotin-nanoMIPs to cells and free doxorubicin (at 100 nM concentration) analyzed by FACS. Prior to incubation with cells, the amount of doxorubicin loaded into both types of nanoMIPs (EGFR and biotin) and added to the cells was adjusted and assessed to be equal by fluorescence and was 95 nM. The control represents cells incubated in the absence of nanoMIPs. Statistical analysis was done by one-way ANOVA. All treated samples are compared to the untreated control; double asterisks indicate $P < 0.01$. (c) Schematic representation of the binding of nanoMIPs to EGFR at on the cell surface, showing the targeted release of doxorubicin.

Furthermore, as shown in **Figure 3b**, doxo-loaded EGFR-nanoMIPs augmented the level of cells in the sub-G1 phase by more than 1.5 times compared to cells treated with doxo-loaded biotin-nanoMIPs or free doxorubicin. These results clearly demonstrate a more-profound cell death in the case of doxo-loaded EGFR-nanoMIPs. To further confirm that the observed effects are due to the specific binding of the nanoMIPs to EGFR, experiments were carried out with both doxo-loaded and unloaded EGFR-nanoMIPs and breast cancer cell lines with high levels (MDA-468) or low levels of EGFR (SKBR-3). Biotin-nanoMIPs were used as negative controls. The results obtained suggest that the EGFR-nanoMIPs mediated delivery of doxorubicin is specific (**Figure S7**) and leads to preferential killing of cells that over-express EGFR (**Figure S7**). Noteworthy is the fact that neither biotin-MIPs nor the double-imprinted doxo-biotin-nanoMIPs affected significantly survival of MDA-MB-468 cells. Furthermore, EGFR-nanoMIPs without doxorubicin did not have any pronounced effect on survival of MDA-MB-468 cells, indicating that it is the targeted delivery of genotoxic drug, doxorubicin, that mediated cell death rather than mere binding of nanoMIPs to EGFR (**Figure S8**).

To directly measure the intracellular levels of doxorubicin in MDA-MB-468 and SKBR-3 cells after the treatment with doxorubicin either bound to EGFR-nanoMIPs or in its free form, we made use of the fact that doxorubicin exhibits autofluorescence at 480 nm, which can be detected with FACS. In fact, EGFR-nanoMIPs loaded with 0.1 μM of doxorubicin caused statistically higher retention of doxorubicin in EGFR high-MDA-MB-468 cells compared to the treatment with free doxorubicin. At the same time, EGFR-nanoMIPs loaded with 0.1 μM of doxorubicin produced much-weaker retention of doxorubicin in EGFR low-SKBR-3 cells, which was comparable to free doxorubicin. These results are consistent with other data, demonstrating that double-imprinted nano-MIPs can be used as specific vehicles for the targeted delivery of drugs (**Figure S9**).

We reasoned that if EGFR-nanoMIPs loaded with doxorubicin caused statistically significant accumulation of the genotoxic drug, then we should also see an increased level of DNA damage in these cells manifested by γ-H2Ax staining. MDA-MB-468 cells were incubated with unloaded or loaded with doxorubicin (0.1 μM) EGFR-MIPs or biotin-MIPs (used as control). Subsequently, cells were stained with antiphosphoH2A.X antibodies followed by confocal microscopy analysis (**Figure S10**). Indeed, we observed statistically significant augmentation of nuclear γ-H2Ax staining when cells were incubated with doxorubicin-loaded EGFR-nanoMIPs but not with doxorubicin-loaded biotin-nanoMIPs.

Finally, we undertook initial attempts to investigate the effect of EGFR-nanoMIPs binding on EGFR signaling. As a consequence of EGFR interaction with its ligand, the receptor undergoes dimerization and subsequent internalization resulting in its accumulation in cytoplasmic lysosomes. Thus, we treated MDA-MB-468 cells with EGFR-MIPs in the presence or absence of EGF (**Figure S12**). We showed that EGFR-MIPs binding with the target receptor even in the

absence of specific ligand caused the accumulation of EGFR in cytoplasm, suggesting that EGFR undergoes endocytosis upon interaction with EGFR-MIPs. Interestingly, we did not observe any significant effect on the downstream activation of EGFR-dependent kinases, e.g. Akt1 (**Figure S11**). However, when cells were incubated with EGFR-nanoMIPs loaded with doxorubicin, we did observe activation of Erk1/2, which is consistent with the previously published data on participation of Erk1/2 in cell stress response.

In summary, in this study, we demonstrated that nanoMIPs prepared via a double-imprinting method against a synthetic epitope of a membrane receptor can specifically recognize a native protein and selectively deliver a drug payload to the corresponding cell targets. As such, nanoMIPs can be considered as a new plausible alternative to conventional antibodies with respect to both the imaging and therapeutic tools against various clinically relevant targets.

ASSOCIATED CONTENT

Supporting Information. The Supporting Information is available free of charge on the ACS Publications website at DOI: 10.1021/acs.nanolett.xxxxxxx. Additional details on experimental methods. Figures showing fluorescence spectra of the nanoMIPs, results of DLS and SPR analysis, confocal microscopy images, FACS analysis of EGFR nanoMIPs, effects of biotinnanoMIPs and EGFR-nano-MIPs loaded and unloaded with doxorubicin, concentration-dependent effect of EGFR-nanoMIPs loaded with different amounts of doxorubicin on survival of MDA-MB-468 cells, and the incorporation levels of intracellular doxorubicin in MDA-468 and SKBR-3 cells.

AUTHOR INFORMATION

Corresponding Author

*E-mail: nick.a.barlev@gmail.com.

*E-mail: sp523@le.ac.uk.

Author Contributions

▽F.C. and L.L. contributed equally to this work.

Notes

The authors declare the following competing financial interest(s): Dr. Canfarotta is employed by MIP Diagnostics Ltd. and, therefore, would like to disclose a competing financial interest.

ACKNOWLEDGMENT

A.P. thanks the UCL Department of Anatomy (Dr. Mark Turmaine) for help with TEM and the NC3Rs for the award of a David Sainsbury Fellowship. A.D., A.P., and N.B. appreciate the support of RSF grant no. 14-15-00816.

REFERENCES

(1) Ecker, D. M.; Jones, S. D.; Levine, H. L. *mAbs* **2015**, *7* (1), 9− 14.

(2) Berg, T. *Angew. Chem., Int. Ed.* **2003**, *42* (22), 2462−2481.

(3) Cochran, A. G. *Curr. Opin. Chem. Biol.* **2001**, *5* (6), 654−659.

(4) Gadek, T. R.; Nicholas, J. B. *Biochem. Pharmacol.* **2003**, *65* (1), 1−8.

(5) Sharma, S. K.; Ramsey, T. M.; Bair, K. W. *Curr. Med. Chem.: Anti-Cancer Agents* **2002**, *2* (2), 311−330.

(6) Hamakubo, T.; Kusano-Arai, O.; Iwanari, H. *Biochim. Biophys. Acta, Proteins Proteomics* **2014**, *1844* (11), 1920−1924.

(7) Doranz, B. J.; Banik, S. S. R. *Genet. Eng. Biotechnol. News* **2015**, *35* (15), 20−21.

(8) Poma, A.; Guerreiro, A.; Whitcombe, M. J.; Piletska, E. V.; Turner, A. P. F.; Piletsky, S. A. *Adv. Funct. Mater.* **2013**, *23* (22), 2821−2827.

(9) Canfarotta, F.; Waters, A.; Sadler, R.; McGill, P.; Guerreiro, A.; Papkovsky, D.; Haupt, A.; Piletsky, S. *Nano Res.* **2016**, *9*, 3463−3477.

(10) Kwapiszewski, R.; Pawlak, S. D.; Adamkiewicz, K. *Targeted Oncology* **2016**, *11*, 739−752.

(11) Hanna, D. L.; Lenz, H. J. *Expert Rev. Clin. Pharmacol*. **2016**, *9* (8), 1091−1108.

(12) Woitok, M.; Klose, D.; Niesen, J.; Richter, W.; Abbas, M.; Stein, C.; Fendel, R.; Bialon, M.; Püttmann, C.; Fischer, R.; Barth, S.; Kolberg, K. *Cancer Lett.* **2016**, *381* (2), 323−330.

(13) Ohba, T.; Toyokawa, G.; Osoegawa, A.; Hirai, F.; Yamaguchi, M.; Taguchi, K. I.; Seto, T.; Takenoyama, M.; Ichinose, Y.; Sugio, K. *Surg. Today* **2016**, *46* (9), 1091−1098.

(14) Canfarotta, F.; Poma, A.; Guerreiro, A.; Piletsky, S. *Nat. Protoc.* **2016**, *11* (3), 443−455.

(15) Poma, A.; Guerreiro, A.; Caygill, S.; Moczko, E.; Piletsky, S. *RSC Adv.* **2014**, *4* (8), 4203−4206.

(16) Ambrosini, S.; Beyazit, S.; Haupt, K.; Tse Sum Bui, B. *Chem. Commun.* **2013**, *49* (60), 6746−6748.

(17) Hoshino, Y.; Koide, H.; Urakami, T.; Kanazawa, H.; Kodama, T.; Oku, N.; Shea, K. J. *J. Am. Chem. Soc.* **2010**, *132* (19), 6644−6645.

(18) Caceres, C.; Canfarotta, F.; Chianella, I.; Pereira, E.; Moczko,́ E.; Esen, C.; Guerreiro, A.; Piletska, E.; Whitcombe, M. J.; Piletsky, S. A. *Analyst* **2016**, *141* (4), 1405−1412.

(19) Moczko, E.; Poma, A.; Guerreiro, A.; Perez De Vargas Sansalvador, I.; Caygill, S.; Canfarotta, F.; Whitcombe, M. J.; Piletsky, S. *Nanoscale* **2013**, *5* (9), 3733−3741.

(20) Basozabal, I.; Guerreiro, A.; Gomez-Caballero, A.; Aranzazu Goicolea, M.; Barrio, R. J. *Biosens. Bioelectron.* **2014**, *58*, 138−144.

(21) Chianella, I.; Guerreiro, A.; Moczko, E.; Caygill, J. S.; Piletska, E. V.; De Vargas Sansalvador, I. M. P.; Whitcombe, M. J.; Piletsky, S. A. *Anal. Chem.* **2013**, *85* (17), 8462−8468.

(22) Shutov, R. V.; Guerreiro, A.; Moczko, E.; De VargasSansalvador, I. P.; Chianella, I.; Whitcombe, M. J.; Piletsky, S. A. *Small* **2014**, *10* (6), 1086−1089.

(23) Garcia-Mutio, D.; Gomez-Caballero, A.; Guerreiro, A.; Piletsky, S.; Goicolea, M. A.; Barrio, R. J. *Sens. Actuators, B* **2016**, *236*, 839.

(24) Garcia-Mutio, D.; Guerreiro, A.; Gomez-Caballero, A.; Gutierrez-Climente, R.; Piletsky, S.; Goicolea, M. A.; Barrio, R. J. *Procedia Eng*. **2015**, *120*, 1132−1136.

(25) Cho, H. S.; Dong, Z.; Pauletti, G. M.; Zhang, J.; Xu, H.; Gu, H.; Wang, L.; Ewing, R. C.; Huth, C.; Wang, F.; Shi, D. *ACS Nano* **2010**, *4* (9), 5398−5404.

(26) Kunath, S.; Panagiotopoulou, M.; Maximilien, J.; Marchyk, N.; Sanger, J.; Haupt, K. *Adv. Healthcare Mater.* **2015**, *4* (9), 1322−1326.

(27) Shinde, S.; El-Schich, Z.; Malakpour, A.; Wan, W.; Dizeyi, N.; Mohammadi, R.; Rurack, K.; Gjörloff Wingren, A.; Sellergren, B. *J. Am. Chem. Soc.* **2015**, *137* (43), 13908−13912.

(28) Yin, D.; Wang, S.; He, Y.; Liu, J.; Zhou, M.; Ouyang, J.; Liu, B.; Chen, H. Y.; Liu, Z. *Chem. Commun.* **2015**, *51* (100), 17696−17699.

(29) Hoshino, Y.; Kodama, T.; Okahata, Y.; Shea, K. J. *J. Am. Chem. Soc.* **2008**, *130* (46), 15242−15243.